Talanta 120 (2014) 218–223

Contents lists available at ScienceDirect

Talanta

journal homepage: www.elsevier.com/locate/talanta

Ultrasensitive enzyme-free electrochemical immunosensor based on hybridization chain reaction triggered double strand DNA@Au nanoparticle tag

Yanqiu Ge [a,b], Jie Wu [a,*], Huangxian Ju [a], Shuo Wu [b,*]

[a] State Key Laboratory of Analytical Chemistry for Life Science, Department of Chemistry, Nanjing University, Nanjing 210093, PR China
[b] School of Chemistry, Dalian University of Technology, Dalian 116023, PR China

ARTICLE INFO

Article history:
Received 9 September 2013
Received in revised form
29 November 2013
Accepted 4 December 2013
Available online 13 December 2013

Keywords:
Electrochemical immunosensor
Signal amplification
Hybridization chain reaction
Carcinoembryonic antigen
Hexaammineruthenium

ABSTRACT

An ultrasensitive enzyme-free electrochemical immunoassay was developed for detection of the fg/mL level carcinoembryonic antigen (CEA) by using a double strand DNA@Au nanoparticle (dsDNA@AuNP) tag and hexaammineruthenium(III) chloride (RuHex) as the electroactive indicator. The dsDNA@AuNP was synthesized by one-pot hybrid polymerization of dsDNA on initiator DNA modified AuNPs via hybridization chain reaction. The immunosensor was prepared by covalently cross-linking capture antibody on chitosan/AuNP nanocomposite modified glass carbon electrode. The AuNPs accelerated the electron transfer and led to high detection sensitivity. With a sandwich-type immunoreaction and a biotin–streptavidin affinity reaction, the dsDNA@AuNP tag was conjugated on the immunocomplex to bring a high amount of RuHex to the electrode surface via electrostatic interaction, resulting in an amplified electrochemical signal. Under optimal conditions, the proposed sensing platform showed a wide linear detection range from 10 fg/mL to 10 ng/mL along with a detection limit of 3.2 fg/mL for CEA. The immunosensor exhibited high sensitivity and good stability, showing a promising application in early cancer diagnosis and could be extended to sensitive electrochemical biosensing of other analytes.

1. Introduction

As is well known, the early clinical diagnosis of cancer can greatly increase the expectation of complete patient recovery. Tumor markers produced by the cancer cells or organs are usually used to signal the presence and progression of a tumor because their levels are associated with the stages of tumors [1,2]. Therefore the development of sensitive and reliable strategies for the determination of cancer-related biomarkers with ultra-low concentration is of great importance in the screening and diagnosis of cancers in the early stage [3]. Various techniques and methods, such as electrochemical [4,5], fluorescent [6], luminescent [7] and colorimetric [8] immunoassays and assays using surface plasmon resonance [9] and quartz crystal microbalance [10], have been designed for ultrasensitive detection of tumor markers. Among these methods, electrochemical techniques have attracted considerable interest due to their high sensitivity, inherent simplicity, portability and low cost [11,12].

In order to achieve ultrasensitive detection, various report probes were designed to generate signals with a high signal-to-noise ratio. The most popular strategy was to load large amounts of reporting molecules, such as enzymes [13], quantum dots [14], metal nanoparticles [15] and electroactive molecules [16], on various micro- or nano-carriers with high surface area, including carbon nanotubes [17,18], graphene [19], magnetic beads [20] and nanoparticles [21]. Due to the advantages of convenient preparation, good biocompatibility and easy functionalization with biomolecules, gold nanoparticles (AuNPs) have been applied as one of the most used nanocarriers [22]. For example, AuNPs can be modified with enzymes or enzyme labeled antibodies to prepare multienzyme nanoprobes and construct enhanced electrochemical immunoassays for low-level proteins [21,23]. However, due to the big size of protein, these probes can only load around 10 enzymes which greatly limit their amplification ability.

Recently, with the rapid advances in DNA design, DNA based signal amplification which employs DNA as amplified indicators attracts great attention. Compared to enzymes, the linear shape of DNA can help to reduce the steric hindrance and be loaded on AuNPs with high amounts. For example, the biobarcode probe invented by Mirkin's group contained around 100 signal oligonucleotide strands on each AuNP, leading to much higher detection sensitivity over other assays using conventional probes [24–26]. In addition, with the introduction of DNA amplification techniques, such as rolling circle amplification (RCA) and hybridization chain reaction (HCR), on-nanoparticle amplification strategies were proposed [27,28]. In these assays, the DNA loaded on AuNP was served

* Corresponding authors. Tel./fax: +86 25 83593593.
E-mail addresses: wujie@nju.edu.cn (J. Wu), wushuo@dlut.edu.cn (S. Wu).

0039-9140/$ - see front matter © 2013 Elsevier B.V. All rights reserved.
http://dx.doi.org/10.1016/j.talanta.2013.12.006

as initiator to in situ trigger the RCA or HCR event, resulting in the linkage of plentiful signal molecules on immunocomplexes and the fg/mL and even sub fg/mL level detection limit of proteins. However, the on-nanoparticle amplifications required strict conditions and long time. In order to simplify the detection, our previous work prepared a three dimensional DNA nanoprobe by HCR [29]. The nanoprobe included an AuNP core and a dsDNA polymerization shell which served as the polylinker for binding of enzymes. By combining the DNA nanoprobe with the enzymatic silver enhancement, the electrochemical immunosensor offered a detection limit down to about 18 molecules.

Here, an ultrasensitive enzyme-free electrochemical immunoassay was developed by using the dsDNA@AuNP tag and hexaammineruthenium(III) chloride (RuHex), $[Ru(NH_3)_6]^{3+}$, as the electroactive indicator. RuHex is a model complex of small DNA intercalator, it could bind to DNA through electrostatic interaction while free of any duplex intercalation [30,31]. Some sensitive assays were developed through attaching and quantifying RuHex on biobarcode tags [31,32]. This work used the dsDNA shell of dsDNA@AuNP tag to capture high amounts of RuHex and sensitively signal the biorecognition event. A chitosan/AuNP (CS/AuNP) nanocomposite film was used to prepare the immunosensor. Both the dsDNA@AuNP tag and AuNPs-promoted electron transfer improved the sensitivity of the immunosensor. The present assay showed a wide linear detection range over 6 orders of magnitude along with a detection limit of 3.2 fg/mL for carcinoembryonic antigen (CEA).

2. Experimental

2.1. Materials and reagents

Mouse monoclonal anti-CEA antibody (Ab1), streptavidin labeled anti-CEA (SA-Ab2) and bovine serum albumin (BSA) were purchased from Beijing Biosynthesis Biotechnology Co., Ltd. (Beijing, China). CEA standard solutions were from CEA ELISA kit, which was supplied by Fujirebio Diagnostics AB (Göteborg, Sweden). Chitosan (CS, ≥95% deacetylation), RuHex and glutaraldehyde (GA, 25% aqueous solution) were purchased from Sigma-Aldrich Chemical Co. (St. Louis, MO). Chloroauric acid ($HAuCl_4 \cdot 4H_2O$) and trisodium citrate were obtained from Shanghai Reagent Co. (Shanghai, China). All other reagents were of analytical grade and used without further purification. Ultrapure water obtained from a Millipore water purification system (≥18 MΩ, Milli-Q, Millipore) was used in the whole assay.

50 mM PBS (pH 7.5) containing 1 M NaCl was used as DNA hybridization buffer for the preparation of dsDNA@AuNP tag. 1 × TE buffer (10 mM Tris, 1 mM EDTA, pH 8.0) was used as the storage buffer for all DNA sequences. The washing buffer was 10 mM PBS (pH 7.4) containing 0.05% (w/v) Tween-20.

The oligonucleotides were purchased from Sangon Biological Engineering Technology & Co. Ltd. (Shanghai, China) and purified using high-performance liquid chromatography. The sequences were shown as following:

Initiator DNA (I-DNA): 5′-**AGTCTAGGATTCGGCGTGGGTTAA** T_{15}-SH-3′
Biotinylated initiator-DNA (B-I-DNA): 5′-Biotin-**AGTCTAGGATTCGGCGTGGG TTAA** T_{15}-SH-3′
Spacer DNA (S-DNA): 5′-SH-T_{15}-3′
Hairpin 1 DNA (H1): 5′-**TTAACCCACGCCGAATCCTAGACT***CAAAGTA*GTCT AGGATTCGGCGTG-3′
Hairpin 2 DNA (H2): 5′-**AGTCTAGGATTCGGCGTG***GGTTAA*CACGCCGAATC CTAGACTACTTTG-3′
Biotinylated DNA1 (B-DNA1): 5′-**TTAACCCACGCCGAATCCTAGACT** T_5-Biotin-3′
Biotinylated DNA2 (B-DNA2): 5′-Biotin-T_5 CACGCCGAATCCTAGACTACTT TG-3′

As shown in Scheme 1(A), I-DNA as well as B-I-DNA was used as initiators to trigger HCR with H1 and H2, and led to dsDNA

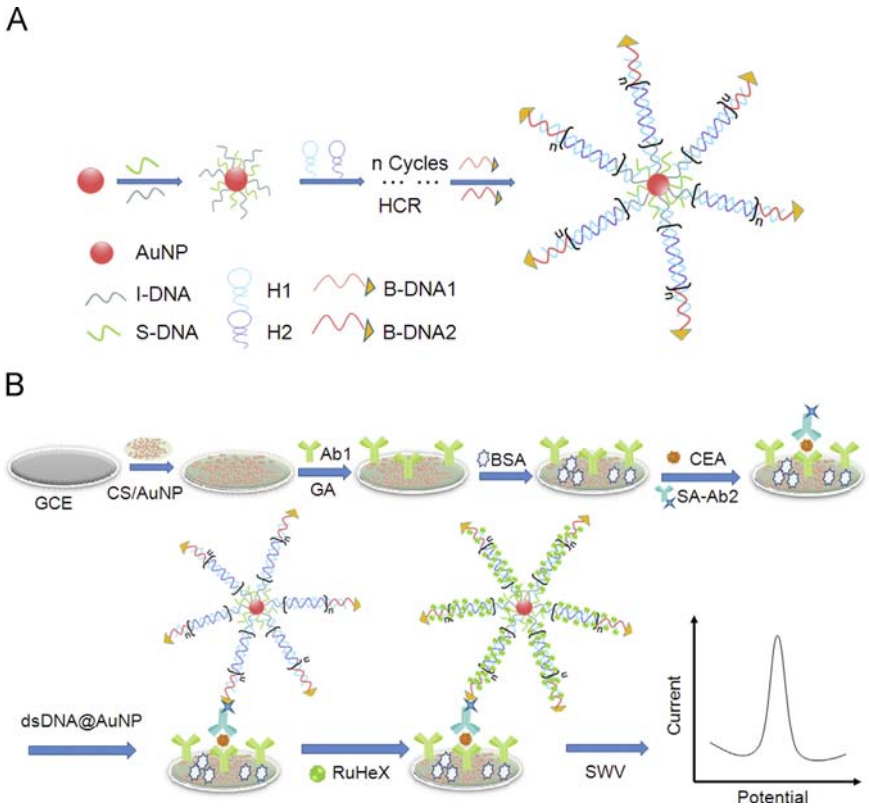

Scheme 1. Schematic diagram of (A) the preparation of dsDNA@AuNP tag and (B) the immunosensor fabrication and electrochemical immunoassay procedure.

polymerization on AuNP surface and immunocomplex, respectively. S-DNA was used as spacer to "stand up" I-DNA and tune its coverage on AuNP surface for achieving high hybridization performance. B-DNA1 and B-DNA2 could bind to the sticky ends of the HCR polymerization to form biotinylated dsDNA@AuNP tag which could further link on the immunocomplex via streptavidin–biotin reaction.

Prior to use, H1 and H2 were heated to 90 °C for 90 s, and then allowed to cool to room temperature for 1 h.

2.2. Apparatus

Square wave voltammetry (SWV) measurements were performed on a CHI 660D electrochemical workstation (CHI, Shanghai, China) at room temperature using a conventional three-electrode system with a modified glassy carbon electrode (GCE) as working electrode, a platinum wire as auxiliary electrode and a saturated Ag/AgCl as reference electrode. Electrochemical impedance spectroscopic (EIS) analysis was performed with an Auto lab PGSTAT12 (Ecochemie) in 0.1 M KCl containing 5 mM $[Fe(CN)_6]^{3-}$/$[Fe(CN)_6]^{4-}$. The ultraviolet-visible (UV–vis) absorption spectra were recorded with a Nanodrop-2000C UV–vis spectrophotometer (Nanodrop, USA). Dynamic light scattering (DLS) measurement was performed by a BI-200SM light scattering apparatus (Brookhaven, U.S.A.).

2.3. Preparation of dsDNA@AuNP

dsDNA@AuNP tag was synthesized according to the previous protocol with slight modification [29]. Briefly, 40 μL of the mixture containing 5 μM I-DNA and 25 μM S-DNA was added into 400 μL of 5.0 nM 13-nm AuNP solution [33] and incubated for 2 h. Then 100 mM PB (pH 7.4) was added to the above mixture to reach the final concentration of 10 mM. The solution was gently shook for 16 h. Small aliquots of 2.0 M NaCl in 10 mM PB were added stepwise to raise the NaCl concentration to 1.0 M, during which a 10-s sonication and a 30-min incubation were required for each additional step of NaCl. The mixture was incubated over 16 h at room temperature. Subsequently, a centrifugation process was performed to remove the excess oligonucleotides and obtain the I-DNA modified AuNPs, which were resuspended in 400 μL 50 mM PB (pH 7.4) containing 1.0 M NaCl. Next, 40 μL of mixture containing 5 μM H1 and H2 was added to the above I-DNA modified AuNP solution and gently shook for 4 h to process the HCR and hybrid polymerization of dsDNA. The excess hairpins were removed by centrifugation. The obtained HCR product was redispersed in 400 μL 50 mM PB containing 1.0 M NaCl. Then, 40 μL of 5 μM B-DNA1 and B-DNA2 was added to the above HCR product and reacted for 40 min to form biotinylated dsDNA@AuNP (Scheme 1 (A)). After removing the excess biotinylated oligos by centrifugation, the obtained dsDNA@AuNP tag was redispersed in 50 mM PB containing 1.0 M NaCl, and stored at 4 °C prior to use.

2.4. Preparation of immunosensor

AuNPs with 13-nm diameter were synthesized according to the previous protocol [33]. Chitosan solution (5%) (w/v) was prepared by dissolving chitosan powder in 50 mM acetic acid. The as-prepared AuNPs, 5% CS, deionized water and 1 M HCl with a volume ratio of 200:20:180:3 were ultrasonically mixed for 2 h to get a homogeneous solution of CS/AuNP.

The GCE was polished to a mirror using 1.0, 0.3 and 0.05 μm alumina slurry (Buehler) followed by rinsing thoroughly with deionized water. After successive sonication in 1:1 nitric acid, acetone and deionized water to remove reducing, organic and aqueous impurities, the electrode was rinsed with water and allowed to dry at room temperature. 5 μL of CS/AuNP was dropped on the GCE and dried in air. Then, 5 μL of 2.5% GA was coated on GCE for 2 h incubation, followed by washing with washing buffer. 5 μL of 0.1 mg/mL Ab1 was dropped onto the GCE to incubate at room temperature for 40 min and 4 °C overnight in a 100% moisture-saturated environment. Subsequently, excess Ab1 was removed with washing buffer. Finally, 5 μL of 2% BSA solution was dropped on the electrode surface and incubated for 1 h at room temperature to block possible remaining active sites against nonspecific adsorption (Scheme 1(B)). After another wash with washing buffer, the immunosensor was obtained and stored at 4 °C before use.

2.5. Measurement procedure

To carry out the immunoassay (Scheme 1(B)), the immunosensor was firstly incubated with 5 μL of CEA standard solution for 30 min at 37 °C [15,29]. After washing with washing buffer, the immunosensor was further incubated with 5 μL of SA-Ab2 (100 μg/mL in 10 mM pH 7.4 PB) for 30 min at 37 °C to form sandwich immunocomplex. Upon another washing step, 5 μL of biotinylated dsDNA@AuNP tag was dropped on the sensor for incubation of 30 min. The sensor was washed with washing buffer and then incubated with 10 μL of 1.25 mM RuHex solution for 20 min. Finally, the SWV measurement was performed from 0 to −0.50 V at 50 mV/s in 10 mM Tris–HCl solution under nitrogen atmosphere environment to record the current response for CEA detection.

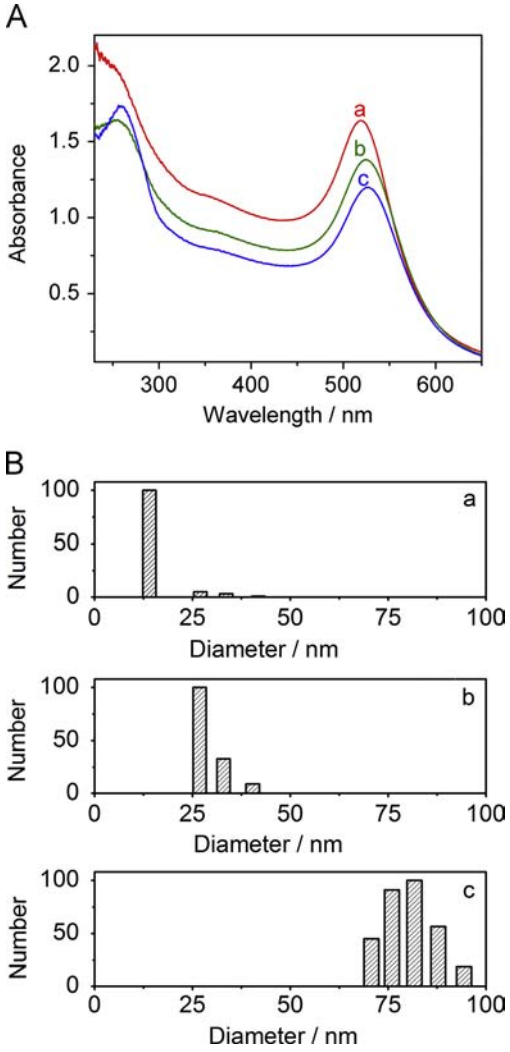

Fig. 1. (A) UV–vis absorption spectra and (B) hydrodynamic diameter of (a) AuNPs, (b) H1@AuNPs, and (c) dsDNA@AuNP tag.

3. Results and discussion

3.1. Characterization of dsDNA@AuNP tag

UV–vis spectra were performed to characterize the formation of dsDNA@AuNP tag. As shown in Fig. 1(A), the size of the AuNPs could be estimated to be 13 nm from its absorption at 519 nm (curve a). After the AuNP modified with I-DNA and further reacted with H1, the UV–vis spectrum of the formed H1@AuNP showed a red shift of the absorption peak to 524 nm and a new absorption at approximately 260 nm due to the adsorption of the DNA strands on AuNP surface (curve b). Compared with H1@AuNP, the absorption peak of the dsDNA@AuNP tag was red shifted to 526 nm, and the absorption at 260 nm was greatly enhanced, indicating the hybrid polymerization of dsDNA on AuNP surface and the successful formation of the dsDNA@AuNP tag.

DLS experiments were performed to characterize the hydrodynamic diameters of AuNPs, H1@AuNP and dsDNA@AuNP. As shown in Fig. 1(B), the average hydrodynamic diameter of AuNPs and H1@AuNP were 14 nm (Fig. 1(B)-(a)) and 27 nm (Fig. 1(B)-(b)), respectively. Compared with H1@AuNP, the average hydrodynamic diameter of dsDNA@AuNP increased to 82 nm (Fig. 1(B)-(c)), suggesting the successful formation of DNA polymerization shell on the AuNP surface. In addition, the DLS results which were in good agreement with the previous work [29] also confirmed that the prepared dsDNA@AuNP tag possessed good dispersity in aqueous media and no aggregations or precipitates emerged.

3.2. EIS characterization of the immunosensor

EIS measurements were performed to obtain the detail information of the modification and detection processes of the immunosensor. In a typical EIS, the diameter of semicircle equals to the electron-transfer resistance, R_{et}, which reflects the electron transfer kinetics of the redox probe at the electrode surface. As shown in Fig. 2, the CS/AuNP modified GCE (CS/AuNP/GCE) (curve b) showed a much smaller R_{et} than bare GCE (curve a), implying that the CS/AuNP nanocomposite was an excellent electric conducting material to accelerate the electron transfer. After the CS/AuNP/GCE modified with Ab1, the protein film increased the impedance, thus showed lager R_{et} (curve c). Similarly, BSA, CEA and SA-Ab2 could all resist the electron-transfer kinetics of the redox probe at the electrode interface, resulting in the increasing impedance of the electrode (curves d–f), which reflected the successful fabrication of the immunosensor and the formation of the sandwich immunocomplex. Subsequent surface incubation with dsDNA@AuNP tag along with RuHex also led to a significant increase in R_{et} (curve g), suggesting the successful conjugation of dsDNA@AuNP tag on the immunocomplex through the biotin–streptavidin affinity reaction.

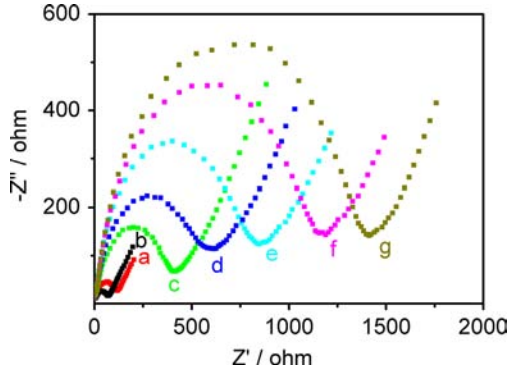

Fig. 2. EIS of (a) bare GCE, (b) CS/AuNP/GCE, (c) *(b)* modified with Ab1, (d) the immunosensor, (e) *(d)* reacted with 1 pg/mL CEA, (f) *(e)* reacted with 100 μg/mL SA-Ab2, (g) *(f)* conjugated with dsDNA@AuNP tag along with RuHex in 0.1 M KCl containing 5 mM $[Fe(CN)_6]^{3-}$/$[Fe(CN)_6]^{4-}$.

3.3. Optimization of detection conditions

After the sandwich immune-recognition, the dsDNA@AuNP tag was easily bound on the target-related immunocomplex *via* biotin–streptavidin affinity reaction to capture the electroactive indicator of RuHex and sensitively signal the biorecognition event. As a result, the redox peak current of RuHex referred to the amounts of dsDNA@AuNP tag, as well as the immunocomplex, on the immunosensor surface, which could be used for immunoassay of protein. Thus, the conditions, such as RuHex concentration and incubation time, that could affect the absorption of RuHex on dsDNA@AuNP tag were optimized (Fig. 3). As shown in Fig. 3(A), the SWV current of RuHex increased sharply with the increasing incubation time and tended to level off after 20 min, indicating the saturation capture of RuHex on the dsDNA shell of dsDNA@AuNP tag. Therefore, an incubation time of 20 min was chosen for the electrostatic absorption of RuHex.

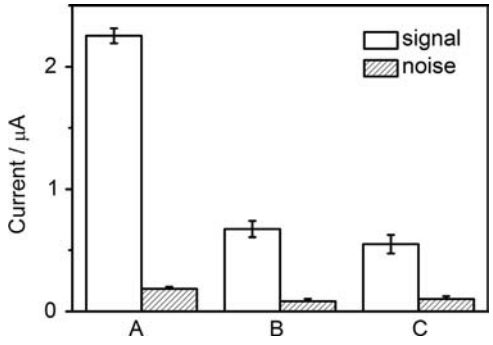

Fig. 4. SWV responses of 100 pg/mL CEA using (A) dsDNA@AuNP tag, (B) H1@AuNP tag, and (C) dsDNA label formed with HCR process along with 1.25 mM RuHex.

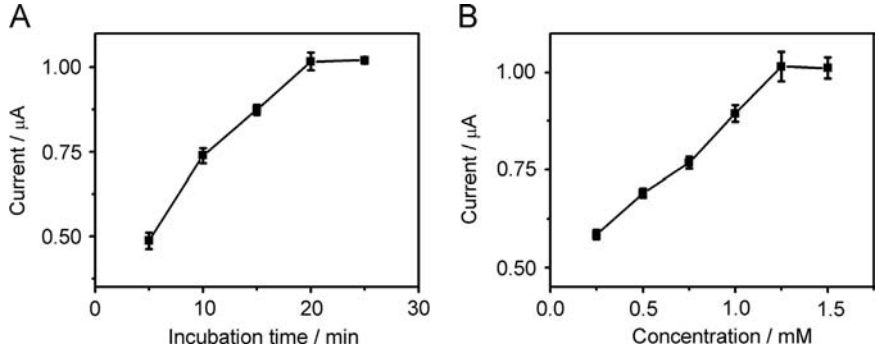

Fig. 3. Effects of (A) the incubation time of RuHex and (B) the RuHex concentration on the current response of 0.1 pg/mL CEA.

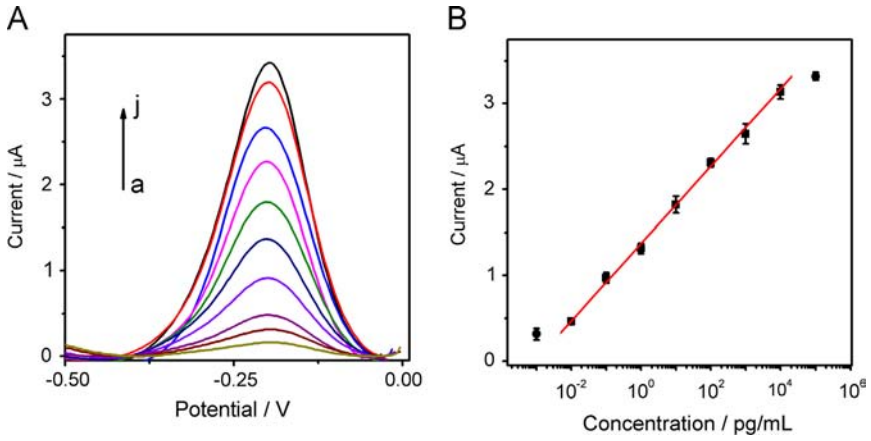

Fig. 5. (A) SWV responses and (B) calibration curve of the proposed method for CEA detection. Curves a–j corresponded to CEA concentrations of 0, 10^{-6}, 10^{-5}, 10^{-4}, 10^{-3}, 10^{-2}, 0.1, 1, 10, 100 ng/mL, respectively.

At the optimized incubation time of 20 min, the effect of the RuHex concentration on the peak current of RuHex on immunosensor was investigated. As shown in Fig. 3(B), with the increase in RuHex concentration from 0.25 to 1.5 mM, the peak current increased and reached the maximum value at 1.25 mM, suggesting that 1.25 mM RuHex was sufficient for the immunoassay. Thus, 1.25 mM RuHex was chosen in the following experiments.

3.4. Amplification property of dsDNA@AuNP tag

In order to evaluate the amplification ability of the proposed dsDNA@AuNP tag, sandwich immunoassays of 100 pg/mL CEA using dsDNA@AuNP and H1@AuNP tag were performed. As shown in Fig. 4, the dsDNA@AuNP tag produced a current response of 2.25 μA, which was 3.4 times higher than that of H1@AuNP tag, along with similar noise. Furthermore, these results have been also compared with those from immunoassay using single dsDNA label. In this immunoassay, B-I-DNA was conjugated on the immunocomplex through biotin–streptavidin reaction to in situ trigger the HCR process and generate a single dsDNA label. Obviously, the dsDNA@AuNP tag produced a stronger current response (4.1 times) than that using a single dsDNA label, leading to a higher signal-to-noise ratio (Fig. 4). These results indicated that the proposed dsDNA@AuNP tag had a good ability to capture higher amount of RuHex and amplify the signal and could be used as an efficient probe for highly sensitive electrochemical immunoassay.

3.5. Analytical performance of the immunosensor

Under optimal conditions, the SWV response increased proportionally with the increasing concentrations of CEA (Fig. 5(A)). The calibration plot showed a good linear relationship between the SWV peak current and the logarithm value of the CEA concentration in the range of 10 fg/mL to 10 ng/mL with a correlation coefficient of 0.9992 under the linear regression equation of $I=0.4505\log[C]+1.3693$ (Fig. 5(B)). The detection limit corresponding to a signal-to-noise ratio of 3 was 3.2 fg/mL, which was much lower than other electrochemical immunoassays reported previously [34–36]. The ultralow detection limit, high sensitivity and wide linear range over 6 orders of magnitude indicated that the proposed electrochemical immunoassay along with the dsDNA@AuNP tag had great potential in immunoassay of low-abundance proteins.

The fabricated immunosensor could be stored at 4 °C before use. After storage of two weeks, the current response of CEA could remain 95% of its initial value, indicating that the proposed immunosensor had acceptable stability.

4. Conclusions

An ultrasensitive enzyme-free electrochemical immunoassay was designed for detection of CEA by using dsDNA@AuNP tag and RuHex as the electroactive indicator. The dsDNA@AuNP tag could be conveniently synthesized by the one-pot hybrid polymerization of dsDNA on initiator DNA modified AuNPs via a HCR process. The high loading of RuHex on dsDNA shell of dsDNA@AuNP tag greatly amplified the detection signal and hence improved the detection sensitivity. The immunosensor was prepared on CS/AuNP nanocomposite modified GCE, in which the AuNPs accelerated the electron transfer. With a sandwich-type immunoassay format, the immunosensor showed a wide linear detection range of over 6 orders of magnitude, low detection limit of 3.2 fg/mL, and good specificity for CEA detection. These features made the proposed immunosensor favorable for the detection of proteins at low level and showed promising application in early cancer diagnosis.

Acknowledgments

We gratefully acknowledge the National Basic Research Program (2010CB732400), the National Natural Science Foundation of China (21105046 and 21275024), PhD Fund for Young Teachers (20110091120012), the Natural Science Foundation of Jiangsu (BK2011552) and the Fundamental Research Funds for the Central Universities (DUT11ZD(G)10 and DUT12LK35).

References

[1] J. Wu, Z. Fu, F. Yan, H.X. Ju, *TrAC Trends* Anal. Chem. 85 (2007) 679–688.
[2] B. Fonslow, B. Stein, K. Webb, T. Xu, J. Choi, S. Park, J. Yates, Nat. Methods 10 (2013) 54–56.
[3] S. Stoeva, J. Lee, J. Smith, S. Rosen, C. Mirkin, J. Am. Chem. Soc. 128 (2006) 8378–8379.
[4] X. Cao, N. Wang, S. Jia, L. Guo, K. Li, Biosens. Bioelectron. 39 (2013) 226–230.
[5] F. Kong, B. Xu, J. Xu, H. Chen, Biosens. Bioelectron. 39 (2013) 177–182.
[6] J.Y. Hou, T.C. Liu, G.F. Lin, Z.X. Li, L.P. Zou, M. Li, Y.S. Wu, Anal. Chim. Acta 734 (2012) 93–98.
[7] L. Zhao, L. Sun, X. Chu, TrAC Trends Anal. Chem. 28 (2009) 404–415.
[8] R.D.L. Rica, M.M. Stevens, Nat. Nanotechnol. 7 (2012) 821–824.
[9] W.C. Law, K.T. Yong, A. Baev, P.N. Prasad, Acs Nano 5 (2011) 4858–4864.
[10] Y. Uludag, I.E. Tothill, Anal. Chem. 84 (2012) 5898–5904.
[11] X.M. Li, X. Yang, S.S. Zhang, TrAC Trends Anal. Chem. 27 (2008) 543–553.
[12] J. Wang, Biosens. Bioelectron. 21 (2006) 1887–1892.
[13] J. Wang, G. Liu, M.R. Jan, J. Am. Chem. Soc. 126 (2004) 3010–3011.
[14] Y.F. Wu, P. Xue, Y.J. Kang, K.M. Hui, Anal. Chem. 85 (2013) 3166–3173.
[15] C.R. Zhao, D.J. Lin, J. Wu, L. Ding, H.X. Ju, F. Yan, Electroanalysis 25 (2013) 1044–1049.
[16] X. Tang, H. Liu, B. Zou, D. Tian, H. Huang, Analyst 137 (2012) 309–311.
[17] R. Malhotra, V. Patel, J.P. Vaque, J.S. Gutkind, J.F. Rusling, Anal. Chem. 82 (2010) 3118–3123.

[18] G.S. Lai, F. Yan, H.X. Ju, Anal. Chem. 81 (2009) 9730–9736.
[19] Y.J. Lai, J. Bai, X.H. Shi, Y.B. Zeng, Y.Z. Xian, J. Hou, L.T. Jin, Talanta 107 (2013) 176–182.
[20] B. Zhang, Y.L. Cui, B.Q. Liu, H.F. Chen, G.N. Chen, D.P. Tang, Biosens. Bioelectron. 35 (2012) 461–465.
[21] A. Ambrosi, M.T. Castaeda, A.J. Killard, M.R. Smyth, S. Alegret, A. Merkoi, Anal. Chem. 79 (2007) 5232–5240.
[22] N. Wangoo, C.R. Suri, G. Shekhawat, Appl. Phys. Lett. 92 (2008) 1331041–1331043.
[23] R. Cui, H. Huang, Z. Yin, D. Gao, J.J. Zhu, Biosens. Bioelectron. 23 (2008) 1666–1673.
[24] S.J. Hurst, A.K.R.L. Jean, C.A. Mirkin, Anal. Chem. 78 (2006) 8313–8318.
[25] R. Duan, X. Zhou, D. Xing, Anal. Chem. 82 (2010) 3099–3103.
[26] D. Zhu, Y. Tang, D. Xing, W.R. Chen, Anal. Chem. 80 (2008) 3566–3571.
[27] B. Zhang, B. Liu, D. Tang, R. Niessner, G. Chen, D. Knopp, Anal. Chem. 84 (2012) 5392–5399.
[28] J. Yan, S. Song, B. Li, Q. Zhang, Q. Huang, H. Zhang, C. Fan, Small 22 (2010) 2520–2525.
[29] L. Tong, J. Wu, J. Li, H. Ju, F. Yan, Analyst 138 (2013) 4870–4876.
[30] A.B. Steel, T.M. Herne, M.J. Tarlov, Anal. Chem. 70 (1998) 4670–4677.
[31] J. Zhang, S.P. Song, L.Y. Zhang, L.H. Wang, H.P. Wu, D. Pan, C.H. Fan, J. Am. Chem. Soc. 128 (2006) 8575–8580.
[32] K. Hu, D. Lan, X. Li, S. Zhang, Anal. Chem. 80 (2008) 9124–9130.
[33] G. Frens, Nat. Phys. Sci. 241 (1973) 20–22.
[34] X.B. Sun, Z.F. Ma, Anal. Chim. Acta 780 (2013) 95–100.
[35] H. Chen, D. Tang, B. Zhang, B. Liu, Y. Cui, G. Chen, Talanta 91 (2012) 95–102.
[36] Y. Cai, H. Li, Y. Li, Y. Zhao, H. Ma, B. Zhu, C. Xu, Q. Wei, D. Wu, B. Du, Biosens. Bioelectron. 36 (2012) 6–11.